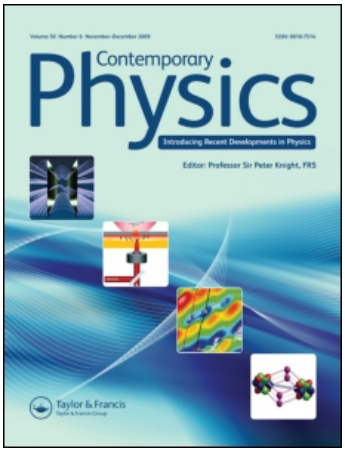


**Contemporary Physics**
Publication details, including instructions for authors and subscription information:
http://www.informaworld.com/smpp/title~content=t713394025

# Antihydrogen for precision tests in physics

M. Charlton[a]; S. Jonsell[a]; L. V. Jørgensen[a]; N. Madsen[a]; D. P. van der Werf[a]
[a] Department of Physics, Swansea University, Swansea, UK

**To cite this Article** Charlton, M. , Jonsell, S. , Jørgensen, L. V. , Madsen, N. and van der Werf, D. P.(2008) 'Antihydrogen for precision tests in physics', Contemporary Physics, 49: 1, 29 — 41
**To link to this Article: DOI:** 10.1080/00107510802038448
**URL:** http://dx.doi.org/10.1080/00107510802038448

*Contemporary Physics*
Vol. 49, No. 1, January–February 2008, 29–41

Taylor & Francis
Taylor & Francis Group

# Antihydrogen for precision tests in physics

M. Charlton*, S. Jonsell, L.V. Jørgensen, N. Madsen and D.P. van der Werf

*Department of Physics, Swansea University, Swansea, UK*

(*Received 14 January 2008; final version received 6 March 2008*)

The creation of atoms of antihydrogen under controlled conditions has opened up a new era in physics with antimatter. We describe the experimental realisation of low energy antihydrogen, via the mixing of carefully prepared clouds of positrons and antiprotons, and some of the progress that has been made in the last few years in characterising properties of the nascent anti-atoms. Ongoing efforts aimed at trapping the anti-atoms in magnetic field minima are discussed. Some of the motivations for undertaking experiments with antihydrogen are presented.

**Keywords:** antihydrogen; CPT; positrons; antiprotons; Penning traps



## 1. Introduction

The prediction by Paul Dirac, in 1930, of the existence of antimatter was one of the most stunning intellectual leaps of 20th century physics. Even before their experimental discovery, Dirac made the following observation on antiparticles:

> '... but if they could be produced experimentally in high vacuum they would be quite stable and amenable to observation.'[1]

This stunning foresight continues to act as a guiding principle for fundamental research with antimatter. The remarkable progress in recent years in making atoms of antihydrogen with low enough kinetic energies to contemplate trapping small quantities of them has been achieved following decades of progress learning how to control their charged constituents. The production and application of low ($\sim$electron-volt) energy positron beams is now routine: antiprotons produced at particle accelerators can now be slowed, trapped, cooled and stored in vacuum in sufficient quantities and for long enough periods to allow them to be combined with positrons under controlled conditions.

Dirac's prediction of the existence of antimatter was soon confirmed from cloud chamber photographs of positrons taken by Anderson [3], and by Blackett and Occhialini [4] who also observed the phenomenon of pair production. Following this, work on the positron was sporadic, mostly focusing on annihilation and on the study of positronium (the quasi-stable electron–positron bound state). The 1970s saw the start of renewed interest in the field when narrow energy width, tunable beams of positrons became available. We will summarise the physics of low energy positrons as relevant to antihydrogen production in Section 3.1.

The discovery of the antiproton had to wait until 1955 and the construction of the 6 GeV Bevatron machine at Lawrence Berkeley Lab, USA [5]. The antiproton has been a workhorse in rich collider physics programmes for many years since. A history of the first 40 years of antiproton physics has been given by Eades and Hartmann [6] who also chart the advances which led to the capture and cooling of antiprotons in Penning traps. This work was pioneered by the group of Gabrielse [7,8] working at low energy antiproton facilities at CERN. These techniques are central to antihydrogen production and are described in some detail in Section 3.1.

Antihydrogen atoms were first produced in the late 1990s [9,10] but at relativistic energies which were not conducive to further experimentation. However, in 2002, two groups working at CERN's Antiproton Decelerator (AD), first ATHENA [11] and then ATRAP [12], announced that they had observed antihydrogen formed at low energies. In this article we will review this work, what has been learnt since, and hint at future directions. Having to assemble your anti-atom before you can study it is obviously not straightforward, so we shall start with the motivations for studying antihydrogen in an effort to elucidate what makes physicists undertake these challenging experiments.

*Corresponding author. Email: m.charlton@swansea.ac.uk

ISSN 0010-7514 print/ISSN 1366-5812 online

DOI: 10.1080/00107510802038448
http://www.informaworld.com

## 2. Theoretical considerations

### 2.1. The CPT theorem and the weak equivalence principle

Amongst the most fundamental properties of the interactions in nature are their symmetries, i.e. the set of operations which leaves the results of an experiment or theory unchanged. In quantum theory symmetries are represented mathematically by operators with eigenvalues which are unchanged by the interactions. The electromagnetic interaction and the strong nuclear force are both invariant under parity (P) transformations, i.e. the transformation which changes the direction of all spatial coordinates,

$$\mathrm{P}(x, y, z) = (-x, -y, -z), \tag{1}$$

in a similar fashion to a mirror image in all three dimensions. Thus, it was believed for many years that parity is a fundamental symmetry of all interactions in nature. In 1956 Lee and Yang challenged this view on the basis of certain decay channels of K-mesons, which could be explained by assuming that parity is violated [13]. They found that no experimental evidence for the parity conservation of the weak force existed, although it had generally been taken for granted. Parity conservation was tested experimentally through the beta-decay of oriented nuclei by Wu et al. in 1957 [14]. They studied the angular distribution of electrons from the beta-decay $^{60}\mathrm{Co} \rightarrow {}^{60}\mathrm{Ni} + e^- + \overline{\nu}_e$. If parity is conserved this distribution should be spherically symmetric, making it identical to its mirror image. However, it was found that for initial states with aligned nuclear spins, electrons were predominantly emitted in the direction opposite to that of the nuclear spin. This showed that the force responsible for beta-decay, the weak nuclear force, does not conserve parity.

Lee and Yang immediately realised that parity violation of the size observed also implied that the weak force violates charge conjugation symmetry (C), which changes all particles into their antiparticles and vice versa. However, some order could be restored by assuming that the weak force is invariant under CP, i.e. the combination of charge conjugation and parity. Thus, the beta-decay of a hypothetical anti-$^{60}$Co nucleus should be the mirror image of the decay of an ordinary $^{60}$Co nucleus. However, in 1964 it was discovered that the weak nuclear force also violates CP in the decay of neutral K-mesons (mesons that we now know contain an s-quark) [15]. The observed decay, $K_L \rightarrow \pi^+\pi^-$, with a branching ratio of about $2 \times 10^{-3}$, is not allowed if CP is conserved. This was a totally unexpected phenomenon. In 2001 it was shown that mesons containing the heavier b-quark also violate CP symmetry [16].

Whereas both P and CP symmetries turn out to be broken in nature, there is so far no known process which violates the combination CPT. Here T stands for time reversal symmetry, i.e. changing the direction of time, for instance when a film is run backwards. It should be emphasised that the conservation of CPT rests on a much firmer foundation than P or CP conservation. According to the rigorously proven CPT theorem, all Lorentz invariant, local, quantum field theories conserve CPT. This is a very strong statement. On the other hand, it is possible to include Lorentz violating terms in a quantum field theory [17]. This entails reintroducing the Newtonian concept of a preferred reference frame. It may also turn out that the 'final theory' unifying all forces is not a local quantum field theory. So far all attempts to unify general relativity and quantum field theory have failed, which leaves the door open to speculation. In the end observations in the form of carefully designed experiments will likely give the final verdict.

Another unsolved puzzle is the absence of large amounts of antimatter in the Universe. It is expected that the Big Bang created matter and antimatter in equal proportion. But, to the benefit of us and everything around us, antimatter is notably absent from our surroundings. One can speculate that antimatter still exists in the Universe, but is separated from us by huge distances. Although this cannot be completely ruled out, searches have revealed no traces of antimatter over distances as large as 20 Mpc [18]. An alternative explanation is that an asymmetry between matter and antimatter has caused some of the former to be left over after all antimatter had annihilated in contact with matter. Although the CP violation of the weak force introduces such an asymmetry it is much too small to explain the matter content of the present Universe. Some additional asymmetry is required, which could be due to CPT violation. It is also notable that searches for evidence of primordal antimatter in the Universe continue today. There are currently two such experiments, PAMELA [19] and the Alpha Magnetic Spectrometer-02 [20], which are particle detectors to be flown in orbit round the Earth to enhance sensitivity to, for instance, anti-nuclei (e.g. the anti-alpha particle). Indeed, PAMELA, which is a satellite-borne instrument, was launched in June 2006 and is already sending data back for analysis.

The CPT theorem can be tested through a comparison of the spectra of hydrogen and antihydrogen. CPT invariance implies that the energy levels of atoms and anti-atoms are identical, such that any difference would be a clear proof of CPT violation.

However, it would still not reveal the exact nature of such an effect, for example, for which force it occurs, whether or not it is connected to a CP violation, or if the CPT violation can be described using a Lorentz-breaking extension of standard quantum field theory. To answer such questions additional theoretical arguments or experimental results would be needed.

A prime candidate for hydrogen/antihydrogen spectroscopic comparisons is the 1S–2S transition, which has been measured in hydrogen to an accuracy of close to one part in $10^{14}$ [21] using two-photon Doppler-free spectroscopy. In this technique the simultaneous absorption of two counter-propagating photons excites the transition, thus cancelling out the first-order Doppler shift caused by the motion of the atom. (See, for example, [22] for a discussion.) It is also notable that a 1S–2S study has been carried out using magnetically trapped hydrogen [23], although so far only to an accuracy of just below one part in $10^{12}$. It has, however, been pointed out [17] that CPT violations arising from certain types of Lorentz-violating quantum field theory would only show up very weakly in the 1S–2S transition. So, despite the fact that this is by far the most accurately measured line for hydrogen, it may not be the best place to search for the failure of CPT symmetry.

Another possible transition to explore is that due to the ground state hyperfine splitting, which, at a frequency around 1.4 GHz in hydrogen, has been measured to about one part in $10^{12}$ [24,25]. This transition has been found to be sensitive to CPT violation in the leading order of coupling terms introduced in Lorentz-violating theories. Possibilities for experiments in this area are actively being considered, particularly by the ASACUSA collaboration [26], who also work at the AD.

Other fundamental matter–antimatter symmetries could be tested using antihydrogen. For instance the acceleration of matter and antimatter in the gravitational field of the Earth could be compared. According to the weak equivalence principle all bodies should undergo the same acceleration in a gravitational field. In Newtonian mechanics this principle follows from the, seemingly coincidental, equality of inertial and gravitational mass, while in general relativity it is a fundamental property. Although an antiproton has essentially the same mass as antihydrogen, its electrical charge makes it less suited for precision tests. Any small electric field would easily give rise to a force which is different between protons and antiprotons, and would mask any difference in the gravitational acceleration. Thus, it is likely that first experiments on the gravitational interaction of antimatter will be performed using neutral species, with antihydrogen as an obvious first candidate.

Several suggestions for antimatter gravity experiments have been made over the years, and most have been reviewed elsewhere [27]. These experiments will demand a great level of control over the anti-atoms, since most require antihydrogen with kinetic energies equivalent to temperatures in the milli-Kelvin range. To see that this is the case, one needs simply to equate the energy needed to raise the mass of the antihydrogen atom in the Earth's gravitational field to a thermal energy given by $k_{\mathrm{B}}T$. Just how far away current research with antihydrogen is from this goal will become apparent in Sections 3 and 4.

### 2.2. *Matter-antimatter interactions*

What happens when matter meets antimatter? Annihilation is of course a likely outcome, but in an atom–anti-atom collision there are more possibilities. For instance, in a hydrogen–antihydrogen collision the possible scattering channels include:

elastic scattering

$$\mathrm{H(1S)} + \overline{\mathrm{H}}\mathrm{(1S)} \rightarrow \mathrm{H(1S)} + \overline{\mathrm{H}}\mathrm{(1S)}, \tag{2}$$

proton–antiproton annihilation

$$\mathrm{H(1S)} + \overline{\mathrm{H}}\mathrm{(1S)} \rightarrow e^{+} + e^{-} + \text{annihilation products}, \tag{3}$$

rearrangement

$$\mathrm{H(1S)} + \overline{\mathrm{H}}\mathrm{(1S)} \rightarrow e^{+}e^{-}\mathrm{(1S)} + p\overline{p}(nl), \tag{4}$$

electron–positron annihilation

$$\mathrm{H(1S)} + \overline{\mathrm{H}}\mathrm{(1S)} \rightarrow p + \overline{p} + 2\gamma, \tag{5}$$

and 'molecule' formation

$$\mathrm{H(1S)} + \overline{\mathrm{H}}\mathrm{(1S)} \rightarrow \mathrm{H}\overline{\mathrm{H}}(vJ). \tag{6}$$

It is clear from the above that rearrangement processes and molecule formation will also ultimately end in annihilation. However, since in these cases the annihilation typically occurs on a timescale which is much longer than for in-flight annihilation during a collision, it is natural to separate these as distinct processes. They could also be regarded as resonances in the annihilation cross-section.

It is interesting to understand the rates and relative probabilities for the various reaction channels. Due to vacuum impurities ordinary atoms will always be present in the experiments, and annihilation with matter is used for detection of antihydrogen. It can

also be desirable to introduce atoms on purpose. For instance, as long as the elastic collision rate is significantly larger than the sum of the rates of all inelastic processes it should be possible to sympathetically cool antihydrogen in a gas of cold atoms. That is, the antihydrogen could cool by transferring kinetic energy to atoms through elastic collisions. Antihydrogen–atom collision experiments would also be a new way to study the strong nuclear force, besides accessing processes which are new and interesting in their own right.

So far we have to rely solely on theoretical data for the collision rates. Calculations have mainly been performed for the antihydrogen–hydrogen and antihydrogen–helium systems. The atom–anti-atom system presents several new challenges compared to ordinary atom–atom collision calculations. Since the Coulomb interaction between the nucleus and the antiproton is attractive they will overlap during a collision. Thus, the strong nuclear force enters the problem, which causes not only annihilation, but may also significantly change the cross-sections for other processes. Another consequence is the large number of open channels. The ground state of the hydrogen–antihydrogen system contains protonium (the bound state, denoted by $p\overline{p}$, of a proton and an antiproton) which has a binding energy of 12.5 keV in its ground state. The protonium states formed in the rearrangement process (4) are therefore highly excited, typically with a principal quantum number $n$ larger than 20.

Calculations show that at low temperatures the two dominating inelastic processes are proton–antiproton annihilation and rearrangement into positronium [28], reactions (3) and (4), respectively. According to the Wigner threshold law the inelastic collision rate approaches a constant value in the limit of vanishing collision energy, while the elastic collision rate goes to zero. Thus, there will always be a minimum energy or temperature below which inelastic processes dominate. Below this temperature sympathetic cooling of antihydrogen will not be possible since too many antiatoms will be lost. According to present calculations this limit is about 1 K for antihydrogen–hydrogen collisions and 10 K for antihydrogen–helium collisions [29,30]. Therefore it is, unfortunately, unlikely that some form of buffer or background gas cooling can be used to lower the temperature/kinetic energy of antihydrogen.

## 3. Experimental realisation

### 3.1. *Antiparticle trapping*

CERN is unique amongst particle physics laboratories in that it has pioneered techniques which allow the *deceleration* of antiprotons. In order to produce antiprotons, a burst of around $10^{13}$ high kinetic energy ($\sim$25 GeV) protons collide with a fixed target. Antiprotons formed, for instance via the reaction $p + p \rightarrow p + p + p + \overline{p}$, can be found amongst the particulate debris. The antiprotons are produced with a wide energy distribution. Those at the peak of this distribution ($\sim 3 \times 10^7$ of them with kinetic energies $\sim$3–4 GeV) are creamed off and fed into the AD ring where they are decelerated and cooled,[2] eventually to a balmy (by CERN's standards) kinetic energy of just 5.3 MeV. Here the antiproton speed is low enough that collisions are dominated by atomic processes, e.g. ionisation. However, 5.3 MeV is still much too energetic for controlled antihydrogen formation, so further energy loss is required.

For the most part the next stage of cooling is achieved via the inefficient, but simple and reliable, technique of slowing down the antiprotons by passing them through a thin foil held in vacuum. The 5.3 MeV antiprotons are ejected from the AD in a burst $\sim$100 ns wide. This pulse arrives at the entrance to the antiproton trapping apparatus, where the thin foil is located. Antiprotons leaving the foil with kinetic energies below about 5 keV (typically just over one per mille of the total – hence the inefficiency) can be dynamically captured into a Penning trap apparatus. Penning traps can store charged particles by use of an axial magnetic field for radial confinement, and an electrostatic well for axial bottling. An example of the type of Penning trap used for the antihydrogen experiments, which consists of a series of appropriately biased cylindrical electrodes immersed in a several Tesla magnetic field, is illustrated in Figure 1.

The trapping sequence is shown schematically in Figure 2. The burst of low energy antiprotons,

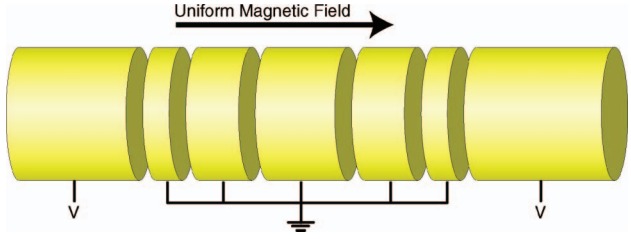


Figure 1. Example of a Penning trap typical of those used in antihydrogen experiments. The particles are confined radially by a strong uniform axial magnetic field. Axially the plasma is held by the electric fields generated by biasing conducting, but individually insulated cylinders (called electrodes) to given voltages ($V$). In the figure the central cylinders have been grounded. By putting, for instance, a positive bias on the two end cylinders (i.e. $V > 0$) positrons can be confined between them. In practice, since more electrodes are needed for all antiparticle manipulations to be possible, the antihydrogen experiments ALPHA, ATHENA and ATRAP use of order fifty individually controllable coaxial electrodes.

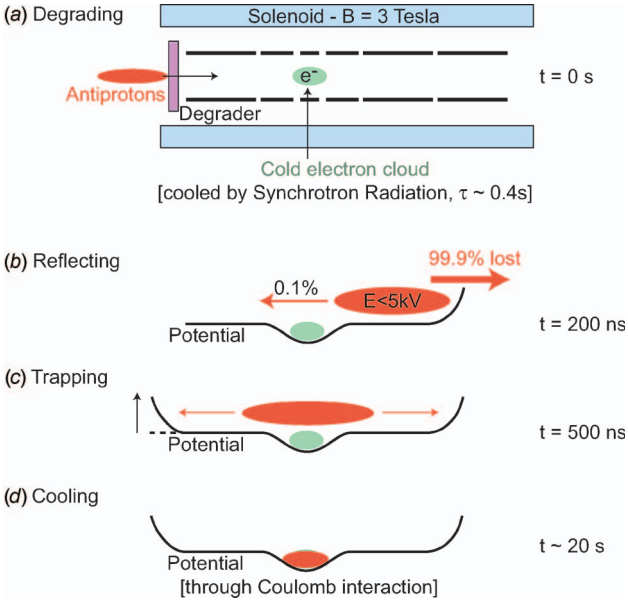


Figure 2. Schematic illustration of antiproton trapping. (*a*) Antiprotons arrive from the Antiproton Decelerator (to the left) with 5.3 MeV kinetic energy and are decelerated in the degrader, which is a metal foil of about 0.1 mm thickness. Electrons have been loaded previously into a centrally located trap in time for them to have cooled to the ambient temperature by emission of synchrotron radiation. (*b*) A wall, made of an electrode charged to high voltage (5 kV in the drawing) is erected before the antiprotons arrive. Antiprotons with low enough energy will be reflected back towards the degrader. (*c*) About 500 ns after the antiprotons arrive the entrance is closed by erecting a similar wall, and the antiprotons are trapped. (*d*) About 20 s later the antiprotons will have cooled down through collisions with the cold (and self-cooling) electrons.

confined by the magnetic field, travels along the axis of the trap where it is reflected by the negative 5 kV voltage applied to the outer electrode. Before the antiprotons can return to the foil (which takes typically 500 ns) it is raised to the same high voltage as the opposite outer electrode. The antiprotons are then trapped.

However, before the antiproton pulse arrives, around $10^8$ electrons are loaded into the central shallow well of the trap. In the strong magnetic field these electrons will typically reach thermal equilibrium with their surroundings on a timescale of a second or so by the emission of synchrotron radiation. The surrounding trap electrodes are usually held at cryogenic temperatures of 20 K and below. The antiprotons pass to-and-fro in the trap, each time traversing the much more numerous electron cloud. The antiprotons lose energy in collision with the electrons (which conveniently radiate the excess away) and are thus sympathetically cooled to the electron, and hence the ambient, temperature. The electrons can be conveniently removed either by exciting their characteristic axial motion,[3] or by quickly lowering their confining potential well, leaving an antiproton cloud containing around $4 \times 10^4$ particles in a volume of $\sim 1\ \mathrm{cm}^3$. The antiprotons are now ready for antihydrogen formation, for whilst the antiproton manipulations were taking place, positrons were being accumulated (by the million) and then transferred to the high B-field region containing the antiprotons.

Positron accumulation follows a similar pattern to the antiprotons, but with one important difference. The positrons are derived as $\beta^+$ particles from a radioactive source (typically from the $^{22}$Na isotope, which is commercially available) and, as such, there is no convenient pulse of them to allow dynamical capture in a trap. Instead, a d.c. beam of positrons is passed through a special Penning trap in which they can lose kinetic energy in collisions with deliberately introduced buffer gas molecules.

The beam itself is derived by a process known as moderation. Most positrons (typically released from the nucleus with kinetic energies of several hundred keV) injected into solid material penetrate deeply into the bulk and annihilate there. However, some, typically a fraction of $10^{-2}$–$10^{-3}$, stop close enough to the surface of the moderator for them to be able to diffuse back. Once at the surface the positron can really behave like an anti-electron and be spontaneously ejected into vacuum. Remarkably, many surfaces have a negative work function for positrons.[4] Furthermore, were the work function to be positive, the positron may have sufficient residual kinetic energy when it reaches the surface to be emitted into vacuum with energies in the electron-volt range. (The latter only occurs for insulating solids in which the slowing down of positrons below band gap energies is inefficient.)

The positron trap is similar to the generic Penning trap illustrated in Figure 1, though it consists of three stages of electrodes with progressively larger diameters immersed in a magnetic field of about 0.15 T. The electrodes are biased to set a trap for the positrons, provided they lose energy in an inelastic collision with the buffer gas, in this case by electronically exciting molecular nitrogen. The gas is fed into the centre of the first stage, which thus has the highest pressure. Once captured, a further excitation of the gas will shuffle the positron into the second stage and then finally into stage three, which has a gas pressure of around $10^{-6}$ mbar. Here the positrons accumulate, and as shown in Figure 3 we can collect over 100 million of them on a 2–3 min timescale. The maths is exactly the same as

capacitor charging (see the caption to Figure 3), with the number of positrons saturating when the rates of accumulation and loss, for instance by annihilation on the buffer gas, are equal.

The positrons are so numerous and dense that they form a plasma. This is not the usual 'textbook' plasma, which is typically electrically neutral, but a plasma made from particles with just one sign of charge. To be a plasma the electrostatic screening length (usually termed the Debye length) must be much smaller than the dimensions of the positron cloud. This occurs in our case after we have accumulated around $10^7$ positrons, which takes about 10 seconds. This non-neutral plasma has an in-built radial electric field which, when combined with the axial magnetic field, means that the equilibrium state of the plasma is one in which it rotates about the axis with a constant angular frequency. Interestingly, the plasma can be further manipulated and compressed using specially adapted electric fields, which cause it to spin faster than its natural rate, and therefore shrink due to the conservation of angular momentum. When desired, the positrons can be readily ejected from the accumulator and sent to the main apparatus, where they are dynamically recaptured, compressed and allowed to cool (like the electrons by emission of synchrotron radiation). In ATHENA, typically 75–100 million positrons, at a density of about $10^{14}$ m$^{-3}$ were available every few minutes for antihydrogen production. Our record has been achieved through stacking of many pulses to achieve a plasma containing over $10^9$ positrons at a density of just under $3 \times 10^{16}$ m$^{-3}$ [31].

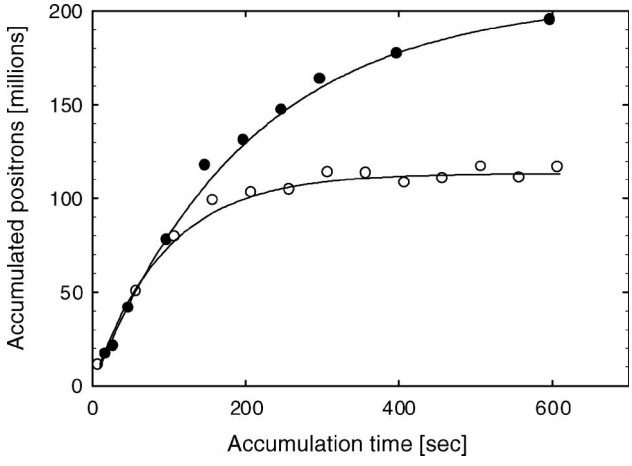


Figure 3. Graph showing the accumulation of positrons with time, $t$. The curves can be fit with the formula, $N = N(\infty)(1 - \exp(-t/\tau))$, where $N(\infty)$ is the saturation limit and $\tau$ is the positron lifetime. The open circles correspond to accumulation in a trap biased statically, whilst the filled circles are when a rotating electric field is employed to shrink the plasma and to help keep it confined. The latter clearly extends $\tau$, which can exceed 100 s, even in the presence of the buffer gas used to promote trapping.

### 3.2. *Recombination*

The positrons and antiprotons are stored in the so-called nested Penning trap arrangement [32] depicted schematically in Figure 4. In order to produce antihydrogen both ATHENA and ATRAP released the trapped antiprotons into their positron clouds. Once the antiprotons have slowed appropriately, antihydrogen formation begins. It is thought that two main processes can lead to antihydrogen production under the conditions of both ATHENA and ATRAP. These are:

radiative recombination

$$\overline{p} + e^+ \rightarrow \overline{\mathrm{H}} + h\nu, \tag{7}$$

and three-body recombination

$$\overline{p} + e^+ + e^+ \rightarrow \overline{\mathrm{H}} + e^+. \tag{8}$$

In the radiative process the excess energy is removed by the emission of a photon. This is an electric dipole-allowed transition and thus favours the formation of deeply bound (typically $n < 10$, where $n$ is the principal quantum number) antihydrogen. It has a weak dependence upon positron temperature, $T_e$, close to $1/T_e^{1/2}$. This process is, however, relatively unlikely since, with timescales for atomic-scale collisions around $10^{-15}$ s and radiative rates at about $10^9$ s$^{-1}$, the probability per collision is about $10^{-6}$.

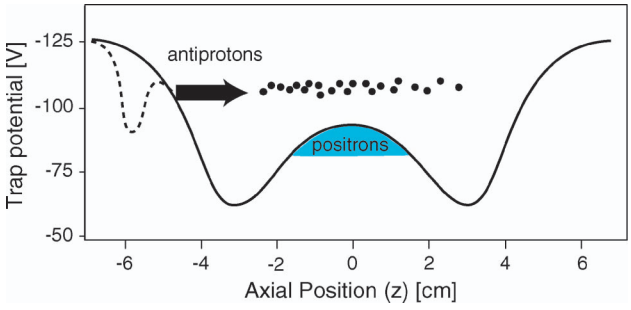


Figure 4. Axial electric potential used for mixing antiprotons and positrons; the so-called nested Penning trap configuration. Note the inverted ordinate axis. Positrons are first loaded into the central well, where they are allowed to cool down to the ambient temperature. Meanwhile, the antiprotons are brought to the injection well, which is indicated by the dashed line. The antiprotons are then launched into the nested potential, and through collisions with the cold positrons they lose energy until they are able to capture a positron and form antihydrogen.

The three-body case occurs when the positron density, $n_e$, is high enough and at low $T_e$. Here the excess kinetic energy is removed by the 'spectator' positron and, as such, this reaction resembles an elastic collision of two positrons in the continuum of the antiproton. Thus, the kinetic energy loss of the positrons is of the order of $k_B T_e$, leading to the formation of very weakly bound states. Indeed these atoms can be so loosely bound that the separation of the positron and antiproton is greater than their cyclotron radii. Such atoms are highly magnetised and behave classically, being guided by the magnetic field. Loosely bound states are also susceptible to field ionisation by the electric fields inherent in the positron plasma-plus-Penning trap configuration. The effect this has on the interpretation of antihydrogen formation data will be discussed further in Section 3.3.

If the antiprotons could be confined indefinitely inside the positron plasma, then they would reach thermal equilibrium at $T_e$. Under these conditions, the relevant length scale of the positron–antiproton interaction is the Thomson radius, $R = e^2/6\pi\epsilon_o k_B T_e$, which is the separation of the pair where the Coulomb interaction energy and the thermal energy $(3k_B T_e/2)$ are equal. Since two positrons are involved, the probability of a positron–antiproton interaction will be $(n_e R^3)^2$. Dividing this by a collision time (which will roughly be $R/v$, with $v$ an average positron speed) then one can see that the rate for reaction (8) should vary as $1/T_e^{9/2}$. Just how closely the conditions of the antihydrogen experiments approach overall thermal equilibrium will have a significant bearing on ensuing observations and will be described further below.

### 3.3. *First observations*

The first controlled production of low energy antihydrogen was achieved by the ATHENA collaboration in 2002 [11]. We have described how the antiparticles were collected and combined; so how was antihydrogen identified? An unambiguous signal is its annihilation, which is comprised of an antiproton annihilation (typically releasing several charged and neutral pions) and a simultaneous (time and position) positron annihilation with an electron into a pair of back-to-back 511 keV $\gamma$-rays. Antihydrogen annihilation ensues following creation of the anti-atom and its migration to the surface of an electrode of the Penning trap. This was the signal used by ATHENA, as depicted in Figure 5, using a purpose-built imaging detector capable of locating the vertex of the antiproton event (with, in this case, the release of three or more charged pions) and the $\gamma$-rays characteristic of positron–electron disappearance. A cut through the cylindrically symmetric detector is shown schematically in Figure 5. The positron–antiproton mixing region was surrounded by a set of silicon strip detectors which could detect the passage of the energetic charged pions. Outside them was a bank of 192 (in 16 rows of 12) CsI scintillator crystals, which could be read out to locate the pair of 511 keV $\gamma$-rays.

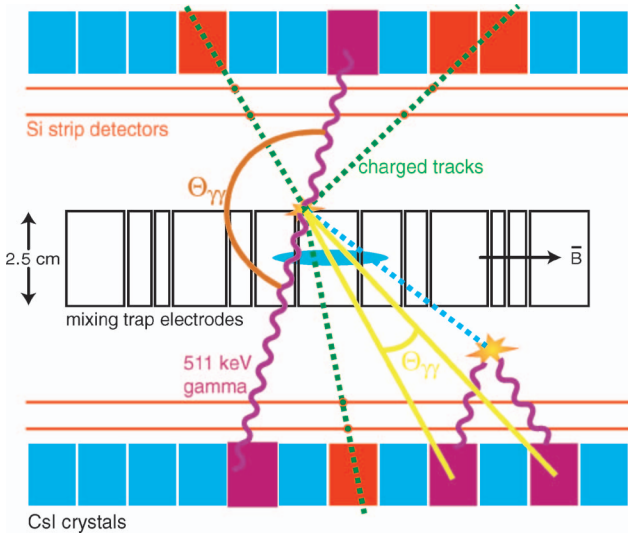


Figure 5. Illustration of the $\gamma - \gamma$ opening angle. The image shows an axial cross-section of the trap and detector. The green lines represent charged pions from an antiproton annihilation event. An annihilating positron results in two back-to-back gammas. The angle between the two points of $\gamma$-ray detection as seen from the antiproton annihilation vertex is the opening angle. The yellow opening angle shows what happens if other events trigger the crystals, for instance from the decay of a neutral pion. When the crystals triggered are geometrically close the opening angle will be small.

Once the antiproton annihilation vertex had been located, the output of the $\gamma$-ray detectors was scanned and any events simultaneous to the antiproton annihilation were plotted versus the cosine of the angle $\theta_{\gamma\gamma}$ between the two $\gamma$-rays. An unambiguous antihydrogen signal would be an event at $\cos(\theta_{\gamma\gamma}) = -1$, corresponding to the back-to-back emission of 511 keV $\gamma$-rays. Figure 6 shows such an opening angle plot with a clear excess of events at $\cos(\theta_{\gamma\gamma}) = -1$. This was the very first sample of antihydrogen atoms produced by ATHENA. Due to space constraints in the apparatus, the $\gamma$-ray detectors used were of limited volume such that their efficiency to register the 511 keV photons was rather small, resulting in only a 0.25% efficiency overall. Thus, the 131 events shown in Figure 6 correspond to over 50,000 antihydrogen atoms in total. (Since then, ATHENA has produced millions of antihydrogen atoms during its many positron–antiproton mixing experiments.)

Figure 6 also shows another important effect. Applying radio-frequency voltage to one of the

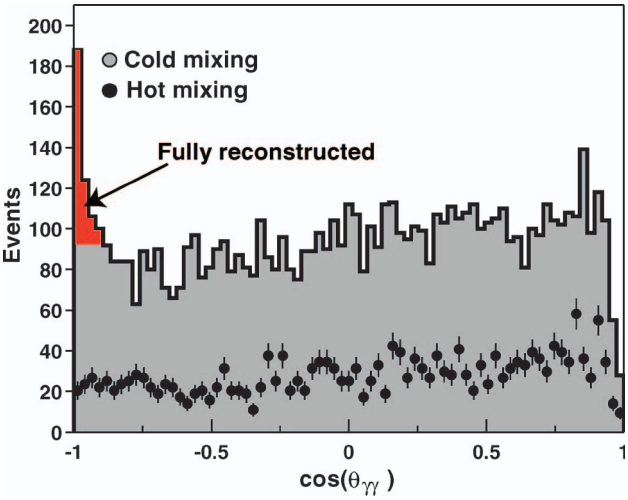


Figure 6. Plot of the cosine of the opening angle of the positron annihilation gammas with respect to the antiproton annihilation point (vertex). The plot shows both cold and hot mixing (see text). The region marked 'fully reconstructed', is the region of excess events of fully reconstructed antihydrogen events, where the opening angle was 180° (within the reconstruction precision). These were the very first data from ATHENA, and the excess here corresponds to 131 ± 22 antihydrogen atoms detected.

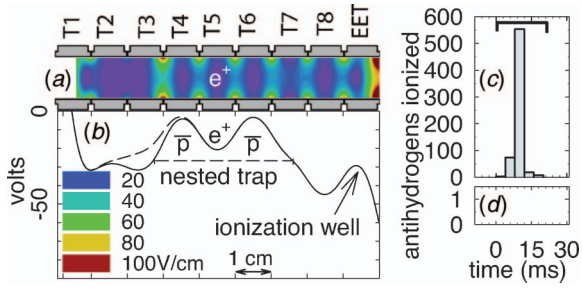


Figure 7. (*a*) Electrode arrangement used in the ATRAP nested Penning trap with a representation of the magnitude of the electric fields present, including the one used to ionise the antihydrogen atoms. (*b*) The on-axis electrical potential for positron interactions with antiprotons (solid line) during which antihydrogen formation took place, with the (dashed line) modification used to launch antiprotons into the well. (*c*) The antiprotons collected by stripping the positron from the antihydrogen in the ionisation well were released from the well during a 20 ms time window. (*d*) No antiprotons were counted in a similar 20 ms window with no positrons present in the nested trap.

electrodes in the nested Penning trap heated the positron cloud (a non-destructive technique was developed to measure by how much) such that antihydrogen formation could be eliminated. This was referred to as hot mixing when compared to the usual cold (i.e. ambient cryogenic) mixing cycles for antihydrogen creation. This provided an important background signal. Painstaking analysis revealed that almost all of the (cold–hot) amplitude was caused by antihydrogen formation, but with $\gamma$-rays detected after scattering, or as a result of decays of neutral fragments produced in the antiproton annihilation.

The ATRAP collaboration used a very different method to detect antihydrogen, relying on the production of weakly bound states via the three-body process; reaction (8). As mentioned in Section 3.2, such weakly bound states can be ionized by electric fields. By applying suitable voltages to create an antiproton trap downstream of their antihydrogen production region, ATRAP were able to identify antihydrogen following its field ionization. A schematic illustration of their nested Penning trap, and their ionization well, can be found in Figure 7, which also shows their first sample of 657 antihydrogen atoms detected in this way [12].

## 4. Where are we now?

Since these pioneering studies, we have learnt more about the antihydrogen that is produced using the nested trap approach, and ATRAP have implemented a new method of antihydrogen production using excited states of positronium as an intermediary.

One feature which seems to have emerged, at least from the ATHENA data, is that antihydrogen is formed sufficiently rapidly that it precedes thermalisation of the antiprotons after their release into the trapped positron cloud. In the ATHENA scenario the antiprotons were injected into the positron cloud with a kinetic energy of around 30 eV. Evidence that antihydrogen formation did not scale with the positron temperature as expected from the (supposed) dominant three-body reaction was soon forthcoming [33]. This was accompanied by observations of antihydrogen formation at rates far in excess of what was expected from the radiative process. Eventually it was realised that the manner of mixing the positrons and antiprotons, whereby the latter pass repeatedly in-and-out of the positron cloud, had a marked influence upon the observed antihydrogen signals. This was noted by Robicheaux [34] who carried out simulations of the antihydrogen formation experiments. He pointed out that the 'arrested' nature of the antihydrogen formation, as the antiprotons repeatedly pass through the positron plasma, *and* since only antihydrogen formed at deep enough binding energies to survive the self-fields of the plasma can leave the plasma, results in major differences between naïve expectations based upon the basic physics of the three-body process.

The antihydrogen detected seems to possess speeds in excess of those expected from the temperature of the positron cloud, as the capture occurs at epithermal antiproton energies. This was discovered in ATHENA

via an analysis of the distribution of antihydrogen annihilations along the axis of the Penning trap [35]. Thus, formation rates should not be expected to depend upon the positron temperature in the manner of antiprotons embedded in a positron plasma of infinite extent. There has been some recent support for this from the aforementioned simulations, and also from experiment. ATHENA could modulate their antihydrogen signal by repeatedly heating their positron cloud using radio-frequency radiation to inhibit formation of the anti-atom. When the positrons self-cooled via the emission of synchrotron radiation in the 3 T magnetic field, the antihydrogen signal was restored. An example of these data is shown in Figure 8. The onset depends upon the positron cooling rate, and the temperature dependence of the antihydrogen formation rate. Thus, the timing scale shown in the figure could be converted into a temperature scale, once the positron cooling rate was factored out. A full analysis [36] found the detected antihydrogen rate to behave as $T_e^{-(1.1 \pm 0.4)}$, in marked contrast to expectations from the three-body reaction. Further modelling work is ongoing to try to shed light on this behaviour.

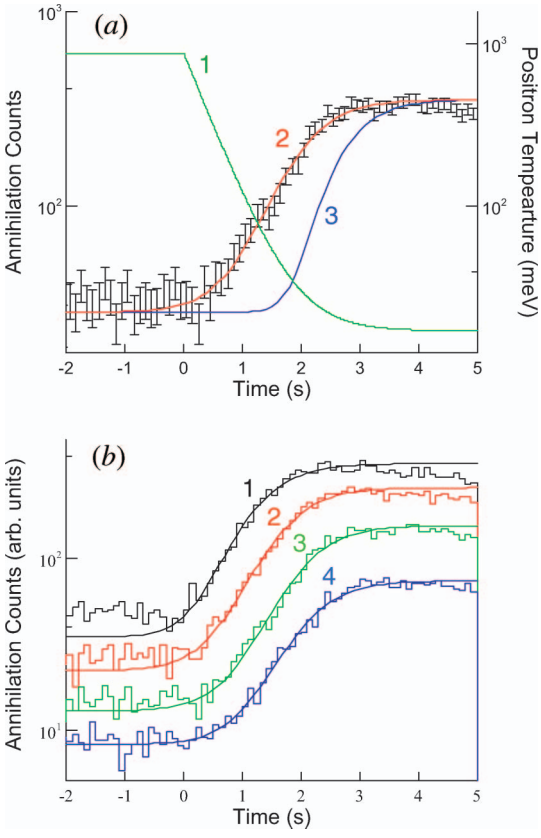


Figure 8. Onset of antihydrogen production after turning the radio-frequency heat off at $t = 0$. (*a*) The data with a positron temperature increase of $\Delta T_e = 870$ meV (plotted with uncertainties). Curve 1: the measured positron temperature evolution. Curve 2: a representative fit, giving the antihydrogen detection rate $R_{\overline{\mathrm{H}}} \propto T_e^{-1.2}$. Curve 3 is the case with $R_{\overline{\mathrm{H}}} \propto T_e^{-9/2}$, similar to expectations for the steady-state three-body reaction. (*b*) The data and fits for different heating temperatures $\Delta T_e$ are compared for 270 meV (curve 1), 400 meV (curve 2), 870 meV (curve 3), and 1150 meV (curve 4). The data sets are vertically displaced for clarity.

The ATRAP collaboration has reported the creation of antihydrogen using a method involving collisions of antiprotons with positronium (the bound state of an electron and a positron) in excited states as [37]:

$$\overline{p} + Ps^* \rightarrow \overline{\mathrm{H}} + e^-. \tag{9}$$

The promise of (9) to form antihydrogen was explored some time ago [38,39], however, more recently, a double Rydberg charge exchange method of achieving the reaction was proposed [40]. The main advantage of using Rydberg atoms is that the cross-section for reaction (9) scales with the positronium principal quantum number, $n_{Ps}$, as $n_{Ps}^4$. With cross-sections for $n_{Ps} = 1$ of order $10^{-19}$ m$^2$, extremely high values of around $10^{-13}$–$10^{-14}$ m$^2$ are to be expected for, say, $n_{Ps} \approx 26$. The experiment was cleverly realised by forming excited state positronium by allowing a trapped cloud of positrons to interact with excited caesium atoms. The latter have strong excitation lines at readily accessible wavelengths, such that a beam of caesium atoms with $n$ values around 37 could be formed. This converted, in collision, about a quarter of the entire positron cloud into positronium atoms in a few tens of seconds of interaction (note that the high cross-section argument given above applies generally to collisions of charged particles with atoms in Rydberg states, and is thus also applicable to the positron–caesium interaction). A fraction of the excited positronium atoms then traversed an antiproton cloud held nearby and were able to form antihydrogen in a highly excited state. The sequence of interactions, including the field ionisation of the resultant weakly bound antihydrogen, is illustrated schematically in Figure 9.

Reaction (9) is an example of a general class of collisions that involve charge transfer. In these interactions it is most likely that the particle which is transferred (in this case the positron) will end up on its new host (i.e. the antiproton) bound by a similar energy to that which it possessed in its original state (the positronium atom). Recalling that the reduced mass of positronium is $0.5m_e$ such that the gross energy levels of positronium are around a half of those of (anti)hydrogen, the binding energy is approximately $6.8/676 \approx 10$ meV for $n_{Ps} = 26$. Thus, the principal

quantum number of the antihydrogen will be around $(13.6/0.01)^{1/2} \approx 37(\approx 26(2^{1/2}))$. This offers advantages over the outcome of the three-body reaction (8) since in the latter there is no direct control over the quantum states formed. A disadvantage is that it is expected that the rate of antihydrogen creation is low in comparison to that of the three-body case, though the antihydrogen will have a low kinetic energy since the internal energies match closely and the recoil electron removes most of the remaining energy. So far ATRAP have only conducted a proof-of-principle experiment in which a few antihydrogen atoms were created via reaction (9). Nevertheless, they have been able to confirm that the production rate was in accord with expectations. Further experimentation is anticipated.

Recently a new antihydrogen experiment, ALPHA, has taken over the reins from ATHENA. Along with ATRAP, ALPHA has the goal of trapping antihydrogen for precision spectroscopy. It is possible to trap certain atoms, if they have low kinetic energies, in positions of magnetic field minima. This is due to the Zeeman effect, which changes the potential energy of an atom in a magnetic field. In particular, those atoms whose potential energy increases with the field (and since total energy is conserved, their kinetic energy must decrease) will be subject to a force which attracts them towards the field minimum in an inhomogeneous field. (Recall that the potential energy, $U$, is related to the magnetic field strength, $B$, as $U = -\mu B$, with $\mu$ the magnetic moment of the atom.) The field minimum can be achieved in three dimensions using a combination of a pair of so-called mirror, or pinch, coils along the axis of the charged particle trap and a multipolar (e.g. quadrupole, hexapole, octupole etc) coil. ALPHA has chosen to use an octupolar geometry and Figure 10 is a photograph of the serpentine-type windings used to achieve this field. ATRAP has a quadrupolar configuration. Figure 11 shows the on-axis magnetic field profile of the ALPHA apparatus, along with a schematic of the electrode system. The axial magnetic minimum is clear, and the radial field due to the octupole coil (not shown) has a similar minimum.

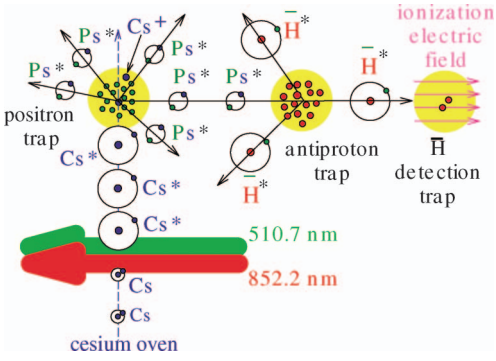


Figure 9. Schematic of ATRAP's antihydrogen formation experiment using excited state positronium [37]. Cs atoms, originating from an oven (bottom) drift through two laser beams that excite them to the desired Rydberg state. The excited atoms continue on their path and collide with a stored plasma of positrons, where they can charge exchange to form excited state positronium ($Ps^*$). Some of the positronium then drifts along the axis of the experiment towards the pre-trapped antiprotons and another charge exchange process then forms antihydrogen. The antihydrogen is detected by stripping the positron off the antiproton with a strong electric field.

In each case the well depth for ground state (i.e. $n = 1$) antihydrogen is $U_w = \mu_B \Delta B$, where $\Delta B$ is the field change between the point of production of the antihydrogen (i.e. close to the axis of the Penning trap) and the electrode walls of the latter and $\mu_B$ is the Bohr magneton. Putting in values, and expressing in terms of temperature, the well depth is about 0.7 K for $\Delta B = 1$ T, which is close to current technical capabilities. Thus, ground state antihydrogen atoms need to be created with equivalent kinetic energies at or below this value if they are to be trapped. Both ALPHA and ATRAP are working to achieve this, an observation which leads directly to our concluding section.

## 5. Conclusions and challenges

A major goal in antimatter physics was achieved in 2002 with the first controlled creation of low energy antihydrogen atoms. Since then further experiments have been performed, providing a number of tantalising clues as to what states of antihydrogen are produced. This has been accompanied by valuable guidance from physics simulations.

Our current understanding is that antihydrogen observation (whether via annihilation on the electrode walls of a Penning trap, or by the field ionisation route)

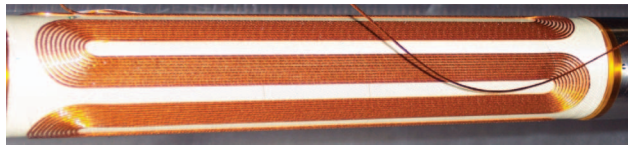

Figure 10. The ALPHA octupole during winding. The wire used is a superconductor with a diameter of about 1 mm, sufficient for the 1100 A currents that run when the magnet is at maximum field. The magnet was wound directly onto the vacuum chamber wall containing the trap electrodes to minimise material between the innermost conductor and the vacuum. This allows for the maximum use of the generated magnetic field. The serpentine structure is fourfold symmetric to create the octupole. Each layer is shifted azimuthally by 45° to avoid generation of an axial field at the ends, where the conductor must turn.

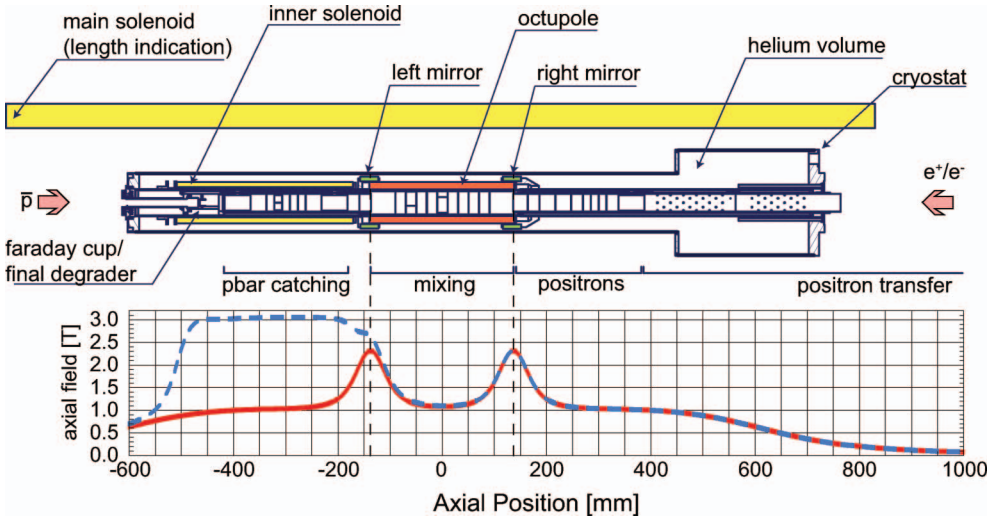


Figure 11. Schematic of the ALPHA apparatus for antihydrogen trapping. The electrodes are housed in a long vacuum chamber onto which the octupole and the mirror coils are wound. This also includes an internal solenoid around the antiproton catching region. This serves to increase the axial field to enhance antiproton trapping. The axial field strength is shown on the lower plot. The octupole field is not visible on this plot as it has zero field on axis and as its main field component is transverse. The dashed line shows the axial field when the internal solenoid is energised.



is a result of a delicate balance between formation of weakly bound states, followed either by their destruction (by ionisation in electric fields or as a result of collisions), or collisional stabilisation before they are liberated from the plasma. Only then can they be detected. As such, the distributions of antihydrogen speeds, binding energies and perhaps even emission angles may be dependent upon plasma density, geometry and temperature. Thus, a major challenge is to understand these effects in order to be able to routinely and efficiently create antihydrogen at low enough kinetic energies and in low enough quantum states that radiative cascade to the ground state is likely. Just how low the kinetic energy needs to be was discussed in the previous section.

In order to perform physics experiments with antihydrogen (for instance comparing the 1S–2S transition with that in hydrogen), it is likely that ground state anti-atoms will need to be trapped. Section 4 contained a brief description of current efforts to trap antihydrogen in a magnetic field minimum. This remains an important goal.

Further into the future, new antihydrogen experiments are planned, such as a measurement of the hyperfine splitting of the ground state using spin-selective techniques combined with an antihydrogen beam. Producing the latter will be challenging. Further away, but now beginning to receive attention, are studies of the gravitational interactions of antimatter. As mentioned in Section 2.1, this will likely require antihydrogen cooled into the milli-Kelvin range or below. Thus, it is unavoidable that new cooling techniques for antiparticles and antihydrogen will need to be developed.

## Notes

1. P.A.M. Dirac, Proc. Roy. Soc. A133 (1931) p. 60. Interestingly, Dirac's hole theory of the positron was introduced as an aside in his paper on 'Quantised singularities in the electromagnetic field' (where the quote at the start of this article can also be found) in which he showed that if magnetic monopoles exist, then electric charge is quantised. His thoughts on antiparticles were also contained in letters he wrote at the time to fellow quantum pioneers. An interesting and informative introduction to the reception of Dirac's relativistic equation for the electron (and its consequences) has been given by Moyer [1]. The discussion of these events in Kragh's scientific biography of Dirac [2] is also an enjoyable read.
2. The deceleration of charged particles in storage rings must be accompanied by reduction of their transverse (to the direction of propagation) energy. This is, in effect, reducing the temperature of the stored particles (hence the term beam cooling is often used) – note the distinction here between kinetic energy and temperature. Lowering transverse components of energy/velocity means that the brightness of the stored particles is preserved, and further stages of deceleration (and cooling) can be facilitated.
3. Charged particles in Penning traps behave like harmonic oscillators and have characteristic frequencies of motion. The axial frequency depends upon trap parameters and the mass of the trapped species. Thus, particles of different masses can be separated by frequency-selective excitation.

4. We are familiar with the concept of the work function from condensed matter physics. The broken symmetry at the surface produces a small electric dipole due to 'leakage' of the electronic charge distribution into vacuum. This dipole is equal and opposite for electrons and positrons and can result in a negative work function for positrons and assures a positive work function for electrons.

## Notes on contributors

Mike Charlton started working on positrons during a final year undergraduate project at UCL in 1977. He did his PhD on positron collisions at UCL and started to think about antihydrogen in the mid-1980s. He has been Professor of Physics at Swansea since 1999 and is currently an EPSRC Senior Research Fellow.

Svante Jonsell obtained his PhD from Uppsala University, Sweden in 2000. Since 2006 he is an EPSRC Advanced Fellow and Lecturer at Swansea University. He works in various areas of atomic theory, presently centering on the formation and interaction of antihydrogen.

Lars Jørgensen obtained his PhD in 1998 from the Technical University of Delft, The Netherlands and he has been working on antihydrogen research and positron accumulation since then. He is currently based at CERN as a Swansea Postdoctoral Research Fellow.

Niels Madsen took his PhD at the University of Aarhus in Denmark in 1998 and has been a Lecturer in Experimental Physics at Swansea University since 2005. His research centres around antihydrogen and low energy plasma physics.

Dirk Peter van der Werf is an RCUK fellow at Swansea University. He received his PhD in 1995 at the University of Groningen, The Netherlands. He has been working on antihydrogen since 1998. His main research interests are antihydrogen and positron physics.

## References


[1] D.F. Moyer, *Evaluations of Dirac's electron, 1928–1932*, Am. J. Phys. 49 (1981), pp. 1055–1062.
[2] H. Kragh, *Dirac: A Scientific Biography*, Cambridge, Cambridge University Press, 1990.
[3] C.D. Anderson, *The positive electron*, Phys. Rev. 43 (1933), pp. 491–494.
[4] P.M.S. Blackett and G.P.S. Occhialini, *Some photographs of the tracks of penetrating radiation*, Proc. Roy. Soc. A 139 (1933), pp. 699–718.
[5] O. Chamberlain et al., *Observation of antiprotons*, Phys Rev. 100 (1955), pp. 947–949.
[6] J. Eades and F.J. Hartmann, *Forty years of antiprotons*, Rev. Mod. Phys. 71 (1999), pp. 373–419.
[7] G. Gabrielse et al. (TRAP collaboration), *First capture of antiprotons in a penning trap: a kiloelectronvolt source*, Phys. Rev. Lett. 57 (1986), pp. 2504–2507.
[8] G. Gabrielse et al. (TRAP collaboration), *Cooling and slowing of trapped antiprotons below 100 meV*, Phys. Rev. Lett. 63 (1989), pp. 1360–1363.
[9] G. Baur et al., *Production of antihydrogen*, Phys. Lett. B 368 (1996), pp. 251–258.
[10] G. Blanford et al., *Observation of atomic antihydrogen*, Phys. Rev. Lett. 80 (1998), pp. 3037–3040.
[11] M. Amoretti et al. (ATHENA collaboration), *Production and detection of cold antihydrogen atoms*, Nature 419 (2002), pp. 456–459.
[12] G. Gabrielse et al. (ATRAP collaboration), *Driven production of cold antihydrogen and the first measured distribution of antihydrogen states*, Phys. Rev. Lett. 89 (2002), p. 0213401.
[13] T.D. Lee and C.N. Yang, *Question of parity conservation in weak interactions*, Phys. Rev. 104 (1956), pp. 254–258.
[14] C.S. Wu et al., *Experimental test of parity conservation in beta decay*, Phys. Rev. 105 (1957), pp. 1413–1415.
[15] J.H. Christenson et al., *Evidence for the 2π decay of the K20 meson*, Phys. Rev. Lett. 13 (1964), pp. 138–140.
[16] B. Aubert et al. (BABAR collaboration), *Measurement of CP-violating asymmetries in B0 decays to CP eigenstates*, Phys. Rev. Lett. 86 (2001), pp. 2515–2522.
[17] R. Bluhm, V.A. Kostelecký, and N. Russell, *CPT and Lorentz tests in hydrogen and antihydrogen*, Phys. Rev. Lett. 82 (1999), pp. 2254–2257.
[18] A.G. Cohen, A. de Rújula, and S.L. Glashow, *A matter–antimatter universe?* Astrophys. J. 495 (1998), pp. 539–549.
[19] PAMELA, http://wizard.roma2.infn.it/pamela/.
[20] Alpha Magnetic Spectrometer, http://ams.cern.ch/.
[21] M. Niering et al., *Measurement of the hydrogen 1S-2S transition frequency by phase coherent comparison with a microwave cesium fountain clock*, Phys. Rev. Lett. 84 (2000), pp. 5496–5499.
[22] C.J. Foot, *Atomic Physics*, Oxford University Press, Oxford, 2005.
[23] C.L. Cesar et al., *Two-photon spectroscopy of trapped atomic hydrogen*, Phys. Rev. Lett. 77 (1996), pp. 255–258.
[24] L. Essen et al., *Frequency of the hydrogen maser*, Nature 229 (1971), pp. 110–111.
[25] D.F. Phillips et al., *Limit on Lorentz and CPT violation of the proton using a hydrogen maser*, Phys. Rev. D 63 (2001), p. 111101.
[26] R.S. Hayano, *Ground-state hyperfine splitting of antihydrogen*, Hyperfine Interact. 172 (2006), pp. 53–62.
[27] M.H. Holzscheiter, M. Charlton, and M.M. Nieto, *The route to ultra-low energy antihydrogen*, Phys. Rep. 402 (2004), pp. 1–101.
[28] S. Jonsell et al., *Stability of hydrogen-antihydrogen mixtures at low energies*, Phys. Rev. A 64 (2001), p. 052712.
[29] S. Jonsell et al., *Strong nuclear force in cold antihydrogen-helium collisions*, Phys. Rev. A 70 (2004), p. 062708.
[30] S. Jonsell, *Low-temperature antihydrogen-atom scattering*, Nucl. Instr. Methods Phys. Res. B 247 (2006), pp. 138–142.

[31] L.V. Jørgensen et al. (ATHENA collaboration), *New source of dense, cryogenic positron plasmas*, Phys. Rev. Lett. 95 (2005), p. 025002.
[32] G. Gabrielse et al., *Possible antihydrogen production using trapped plasmas*, Hyperfine Interact. 44 (1989), pp. 287–294.
[33] M. Amoretti et al. (ATHENA collaboration), *Antihydrogen production temperature dependence*, Phys. Lett. B 583 (2004), pp. 59–67.
[34] F. Robicheaux, *Simulations of antihydrogen formation*, Phys. Rev. A 70 (2004), p. 022510.
[35] N. Madsen et al. (ATHENA collaboration), *Spatial distribution of cold antihydrogen formation*, Phys. Rev. Lett. 94 (2005), p. 033403.
[36] M.C. Fujiwara et al. (ATHENA collaboration), submitted for publication.
[37] C.H. Storry et al. (ATRAP collaboration), *First laser-controlled antihydrogen production*, Phys. Rev. Lett. 93 (2004), p. 263401.
[38] M. Charlton, *Antihydrogen production in collisions of antiprotons with excited states of positronium*, Phys. Lett. A 143 (1990), pp. 143–146.
[39] B.I. Deutch et al., *Antihydrogen synthesis by the reaction of antiprotons with excited state positronium atoms*, Hyperfine Interact. 76 (1993), pp. 151–161.
[40] E.A. Hessels, D.M. Homan, and M.J. Cavagnero, *Two-stage Rydberg charge exchange: an efficient method for production of antihydrogen*, Phys. Rev. A 57 (1998), pp. 1668–1671.